doi.org/10.26434/chemrxiv.13296878.v1

A Low-Cost Mechatronic System for Sol-Gel Spraypyrolysis Technique

Martin E. Oviedo, Fernando Alvira, Agustin Apaolaza, Juan F. Martiarena, Matías R. Tejerina

Submitted date: 28/11/2020 • Posted date: 01/12/2020

Citation information: Oviedo, Martin E.; Alvira, Fernando; Apaolaza, Agustin; Martiarena, Juan F.; Tejerina, Matías R. (2020): A Low-Cost Mechatronic System for Sol-Gel Spraypyrolysis Technique. ChemRxiv. Preprint. https://doi.org/10.26434/chemrxiv.13296878.v1

This work presents a design of a low-cost spray pyrolysis automatized system which allows to manufacture high quality thin films. In particular, the thermal component of this instrument is modelled in different operation conditions, analyzed, and controlled. Also, different configurations for the whole instrument are analyzed.

File list (1)

Paper para arXiv.pdf (688.61 KiB) view on ChemRxiv • download file

A low-cost mechatronic system for sol-gel spray-pyrolysis technique

Martín Oviedo
Univerisad Nacional de Quilmes, Department of Science and Technology, Laboratorio de Instrumentación Automatización y Control, Roque Saenz Peña 352, Buenos Aires, Argentina Zip: 1876, eliasoviedo1718@gmail.com

Fernando Alvira
Univerisad Nacional de Quilmes, Department of Science and Technology, Laboratorio de Instrumentación Automatización y Control, Roque Saenz Peña 352, Buenos Aires, Argentina Zip: 1876, fernando.alvira@unq.edu.ar

Agustín Apaolaza
Departamento de Física, Facultad de Ciencias Exactas, Universidad Nacional de La Plata
agustinapaolaza@hotmail.com

Juan F. Martiarena
Facultad de Ingeniería Univesidad Nacional de La Plata La Plata, Buenos Aires, Argentina
juanf.martiarena@ing.unlp.edu.ar

Matías R. Tejerina
Centro de Tecnología de Recursos Minerales y Cerámica Consejo Nacional de Invesigaciones Científicas y Técnicas Gonnet, Buenos Aires, Argentina
matiast@cetmic.unlp.edu.ar

***Abstract*—This work presents a design of a low-cost spray pyrolysis automatized system which allows to manufacture high quality thin films. In particular, the thermal component of this instrument is modelled in different operation conditions, analyzed, and controlled. Also, different configurations for the whole instrument are analyzed.**

Keywords—spray pyrolysis, temperature control, mechatronic system, high quality films

I. Introduction

Spray pyrolysis is a low-cost method employed to manufacture high quality ceramic nano and microlayers. In this method, the host material is maintained at relatively high and constant temperature (about 400°C or more) and a gel solution is sprayed over it. The pulverized droplets of a metallic ion reach the heated surface, those are sintered. In this way solid agglomeration of crystallites conforms a semiconductor ceramic layer [1-3].

The development of spray pyrolysis automatized system constitutes a technological challenge. It mainly requires the control of positions of the spray nozzle and substrate, its temperature and quality of flow sprayed. However, this kind of system opens the door to develop high quality semiconductor thin films for scientific research and technological applications [4-5]. In this paper, we describe some considerations of the different components of this mechatronic system and present a scheme of the automatization of the complete process. We analyze the dynamics of a homemade thermal component and variations of the physical model, which was in a first configuration, controlled with a commercial PID controller, and finally, a low-cost controller Arduino is proposed to integrate the multiple subsystem components. The contribution of this work is to show a possible configuration for a low-cost and automatized spray pyrolysis system.

II. Spray Pyrolysis System.

A spray pyrolysis system requires the application of a pulverized solution over a heated substrate (Figure 1(a)). The solution droplets undergo several reactions (evaporation, condensation, drying, and thermohydrolysis) to precipitate nanoparticles at operating temperature. As a result, a thin film of a metallic oxide is generated. In Figure 1(b) is presented a scheme of the laboratory system that we employ to manufacture thin films. The specific design is aimed to use a conventional glass slide (7x2 cm) as a substrate over an aluminum plate holder. The design temperature of the heated

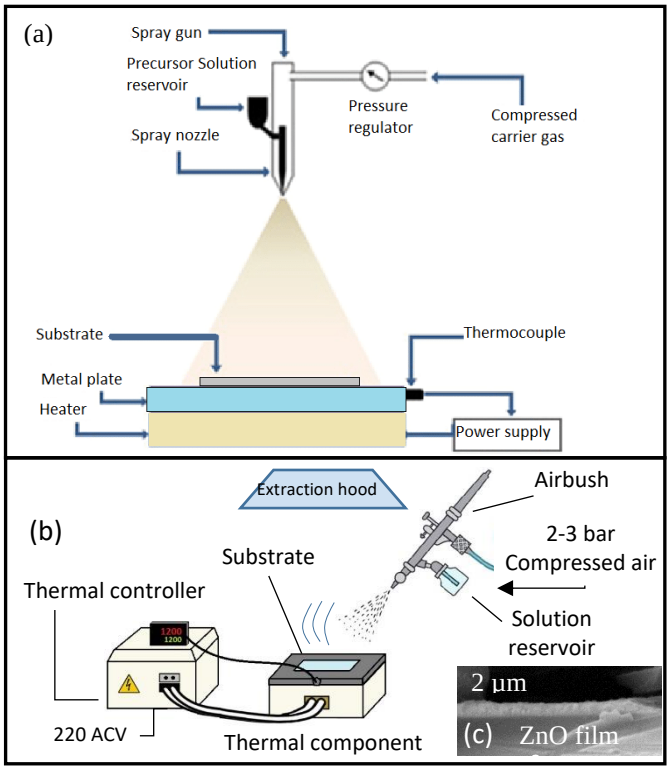

substrate is 450°C. The distance between the substrate and the spray nozzle was about 0.2 m. In this configuration, the solution is manually and intermittently sprayed over a glass substrate employing a commercial airbrush with compressed air at 2-3

Figure 1(a) Spray pyrolysis system (b) Manual system operated in our laboratory (c) A ZnO thin film obtained using this system.

bar and 40 mL of solution (Zinc salt diluted in ethanol). A ZnO film obtained with the described system is presented in Figure 1 (c), the image was taken by a Scanning Electronic Microscope.

The deposition process is carried out within a laboratory fume hood because of toxic solvent evaporation and takes around 40 minutes. The solution is intermittently sprayed because a continuous application generates a decrease of the substrate operation temperature and the particle formation process can be disrupted. Also, after deposition of about 30 ml of solution, the particles of metallic oxide are usually accumulated around the nozzle outlet producing a partial obturate of the outlet hole that modifies the flow and thus the deposition conditions. In the mentioned conditions, the process needs operator implementation and supervision. These make valuable an automatized process, which controls simultaneously the temperature of the substrate, airflow and pulverized cone, and any other variable like substrate-nozzle distance to ensure an adequate result without continuous operator observation.

A. Thermal component

As mentioned before, an important specification is to set the substrate holder temperature at a constant value of 450±1°C. It should be considered that this parameter will be affected by almost two relevant perturbations: the flow of pulverized solution over the substrate and the air extraction of the extraction hood. The first is dominated by evaporation of the solvent and convection, and the second only by convection. So, it is necessary an interactive control of the subsystem. To achieve this, it is proposed an electrical resistance embedded in ceramics as actuator and over this, was mounted and aluminum substrate holder, as presented in Figure 2 (a). The temperature of the holder is measured by a K type thermocouple fixed inside an aluminum screw-threaded inside the holder. The electrical resistance has an electrical power consumption of 500 W and connected to a solid-state relay (NOVUS SSR 4840) with an input voltage ranged within 3-32V DC. This relay supplies AC 220 V to the electrical resistance.

In a first configuration, this thermal subsystem was controlled by a PID NOVUS 1200. In this, it was set in mode ON/OFF and in mode Autotune. The substrate temperature as a function of time is presented in Figure 2(b). The homogenous ZnO film shown in Figure 1(c) was made using the second setting mode of the controller.

The plant of the thermal component is formed by the aluminum plate and the ceramic resistance. The dynamics of this subsystem are low compared with the others, so the first approximation is considered the whole ceramic+aluminum as the plant, which is embedded in a high porosity ceramic block, so the set is assumed to be thermally isolated on the underside.The output is the temperature of the aluminum plate (10x6x1cm), assumed equal to the substrate.

First, a mathematical model was implemented. This should consider the thermal dynamics of the aluminum holder and the resistance embedded in the ceramic. For the aluminum plate, the energy balance equation can be written as follows:

$$P - \dot{Q_{conv}} = C\frac{dT}{dt} \qquad (1)$$

Where C is the heat capacity, P is the electrical power supplied to the resistance by mass unit, Q_{conv} is the energy loss rate by

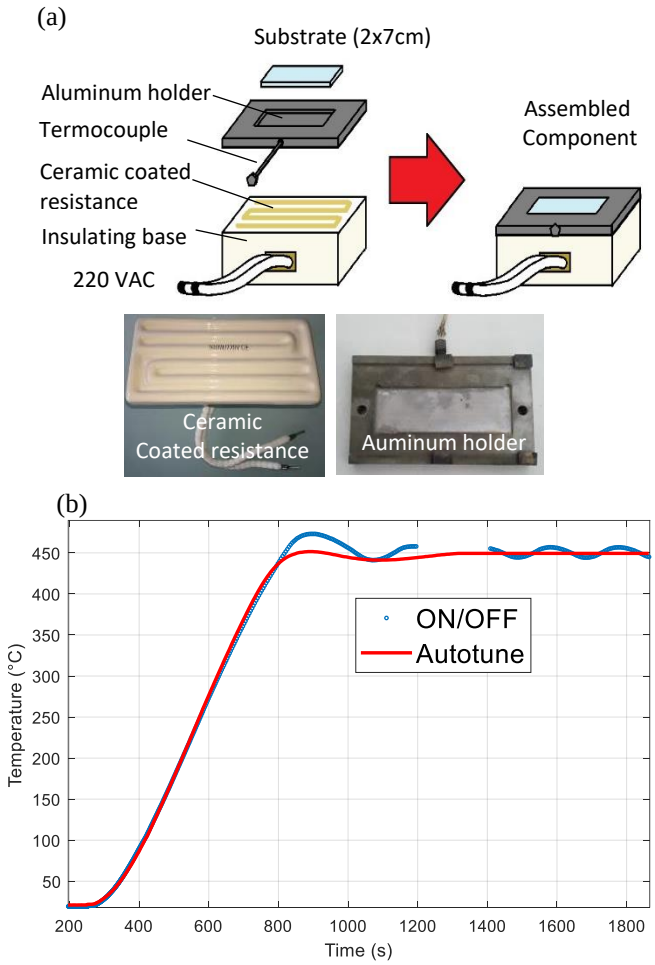

Figure 2 (a) Thermal component mounting (b) Temperature of the sample holder as a function of time.

free convection. Radiation and conduction losses are not considered.

The electrical power is a constant parameter and is the control action. The action of this parameter is influenced by the dynamics of the ceramic resistance, in which the plate is sustained. The heat transfer through the ceramic can be assumed in the same way as in the case of the aluminum plate, by considering the different properties of this material.

If it is assumed not energy exchange between the ceramic and the surrounding. The energy balance of the ceramic during a differential of time is expressed as follows.

$$CdT = (\dot{q}_{bi} - \dot{q}_{bs})dt \qquad (2)$$

Where C is the thermal capacity of the ceramic, $\dot{q}_{bi}$ is the thermal flux gained and $\dot{q}_{bs}$ is the thermal flux lost by the ceramic. The power transmitted to aluminum is determined by considering the ceramic model.

Reordering and replacing Equation 1 in Equation 2, we get the expression in Equation 3.

$$\frac{dT}{dt} = \frac{P}{C_{eq}} - \frac{k_{eq}A}{C_{eq}}(T - T_0) \quad (3)$$

Where it is assumed $P = \dot{q}_{bi}$, the ceramic inlet power is the power of the resistance and $\dot{q}_{bi} = -kA(T - T_0)/C$, the output power of the system which is mainly due to natural convection.

The equivalent heat capacity C_{eq} is obtained by the addition of $C_{Al}=c_{Al}\cdot m_{Al}$ and $C_c=c_c\cdot m_c$.

The parameter k_{eq} is the heat convection coefficient for convection. This parameter depends on temperature, for our analysis is set constant between 0.2 and 0.8 W/K·m^2[6], and A the area of convection, in this case, is 170 cm^2.

The model which give raise to Equation 4 represents a state equation, from which the transfer function between the state T and the action control P can be obtained in Laplace space, as follows [7]:

$$\frac{T(s)}{P(s)} = \frac{\frac{1}{C}}{s + \frac{kA}{C}} \quad (4)$$

In Table I we summarize the value of the different parameters employed in the model.

Symbol	Parameter	Value
Tr	Reference temperature	450°C
T_{inf}	Ambient temperature	20°C
P	Power supplied by resistance	440 W
m_{Al}	Aluminum plate mass	0.250 Kg
m_c	Ceramic mass	0.505 Kg
c_{Al}	Specific heat of aluminum	880 J /Kg °C
c_c	Specific heat of ceramic	921 J/Kg °C
$C=C_{eq}$	Equivalent Heat capacity	698 J/°C
A	Area of upper surface of the thermal component	$1.7\cdot10^{-2}$ m^2
K	Heat convection coefficient	0.2 to 0.8 W/°C·m^2

Table I. Description of used parameter

The first-order model presented in Equation 4 has a response velocity represented by the position of the denominator root (pole) in the complex plane. To analyze the frequency response, it is presented in Figure 3 the Bode diagram of the plant. In this, it can be appreciated that the bandwidth is about $2\cdot10^{-5}$ rad/s. Figure 3(a) shows that the bandwidth of the system depends on the selected parameter k_{eq}, and it is between $3 \cdot 10^{-3}$ and $1 \cdot 10^{-2}$.

The response to a stepped input is seen in Figure 5, also parameterized according to k_{eq}. In this figure is shown the output signal to: (a) an open-loop configuration, (b) feedback employing ON/OFF controller, and (c) feedback employing a PID controller. For all these configurations, when k is increased, the slope of the temperature is decreased, as expected. PID and ON/OFF controllers show a reasonable response and simulate the experimental behavior measured presented in Figure 2(b). The PID parameters were obtained using Ziegler-Nichols method (P=0.81, I=0.01, D=0). The differences can be attributed to the variation of k parameter

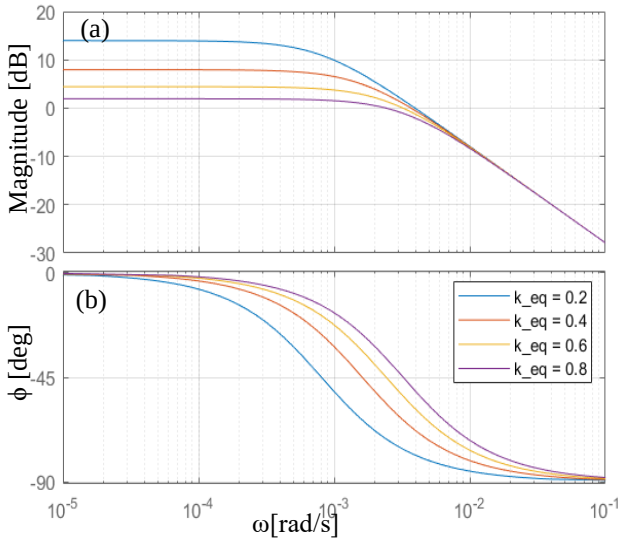

Figure 3. Bode diagram of the plant for different values of k_{eq}

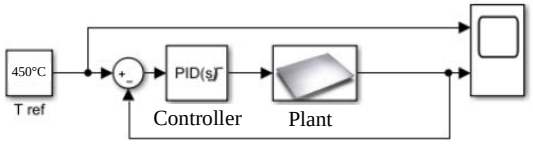

Figure 4. Block diagrams of the thermal controller.

and specific heat with temperature and not considered thermal losses like radiation and conduction.

To simulate the control of the thermal component we generate the diagram of blocks presented in Figure 4.

By making the analysis shown above, we have made the open loop measurement of the plant presented in Figure 2(a) suppling 220 V and the resistance embedded in ceramic failed when it reached about 520°C. Then, another type of 500W resistance was designed and evaluated in open-loop measurement. In Figure 6(a) it is shown the elastic resistance in a specially designed ceramic mount. Over this, the aluminum holder was placed to perform an open-loop measurement and directly retrieve plant parameters. By considering the following transfer function presented in Equation 6, we obtained the following plant parameters: K=1.40±0.01, t=38 ±1 s, ϒ=300 to 450 s.

$$G(s) = \frac{Ke^{-ts}}{\Upsilon s+1} \quad (6)$$

To determine PID parameters of the controller we used Ziegler-Nichols method (P= 6.7 I= 76.0 D= 19.0). In Figure 6(b) we plotted the simulated (for different characteristic time

values) and the experimental open loop response. In Figure 6(c) we present the output signal of the close loop response (for γ = 300 s) with the mentioned PID controller. Due to operational difficulties we could not measure experimental close loop response using NOVUS controller and experimental perturbations due to spraying. The first will be similar to that presented in Figure 2(b) and the second is qualitatively known by us from our experience.

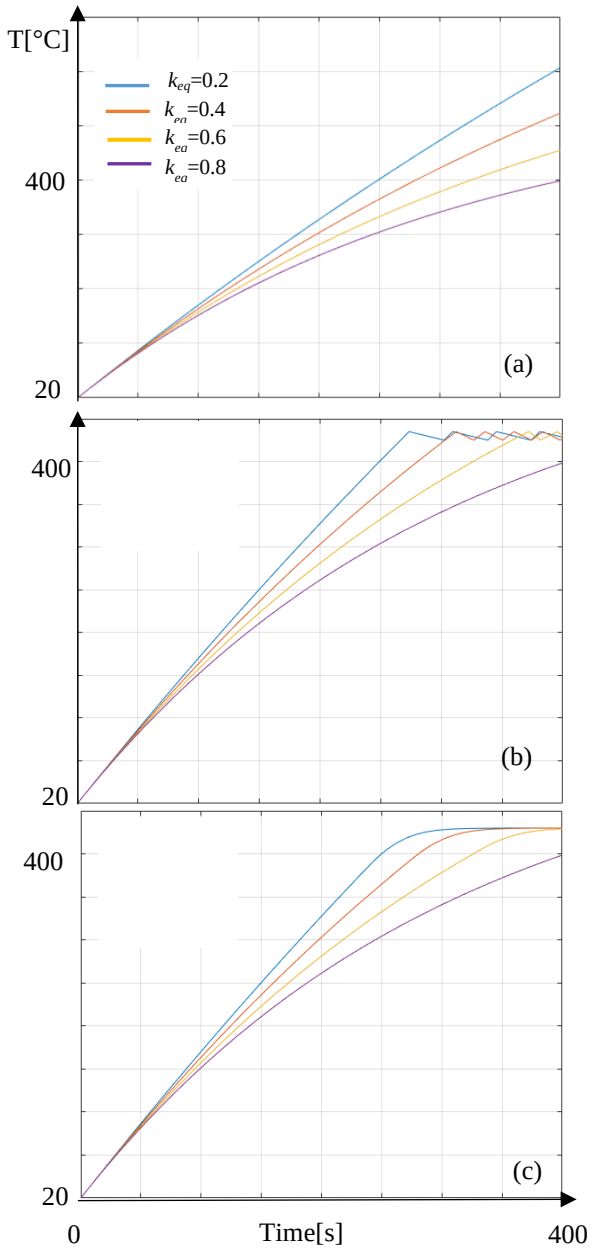

Figure 5. Step response for different values of k_{eq} (a) open-loop (b) using a ON/OFF controller (c) using a PID controller.

So we analyze the operation conditions, the perturbation to substrate temperature due to convection of spraying can be expressed by equation 6. Heat losses due to evaporation can be neglected because of the low flow rate of the solution [8].

$$\frac{dQ}{dt} = hA_s(T_s - T_{\text{inf}}) \tag{7}$$

Where h is the convection coefficient, A_s is the area of contact with the fluid (in this case is about 0.002 m^2), T_s is the temperature of the substrate (450°C) and T_{inf} is the fluid temperature away from the substrate (ambient temperature 25°C). For spray cooling, a convection coefficient of 30±10 W/K·m^2 is estimated [9], so the loss of heat during spraying

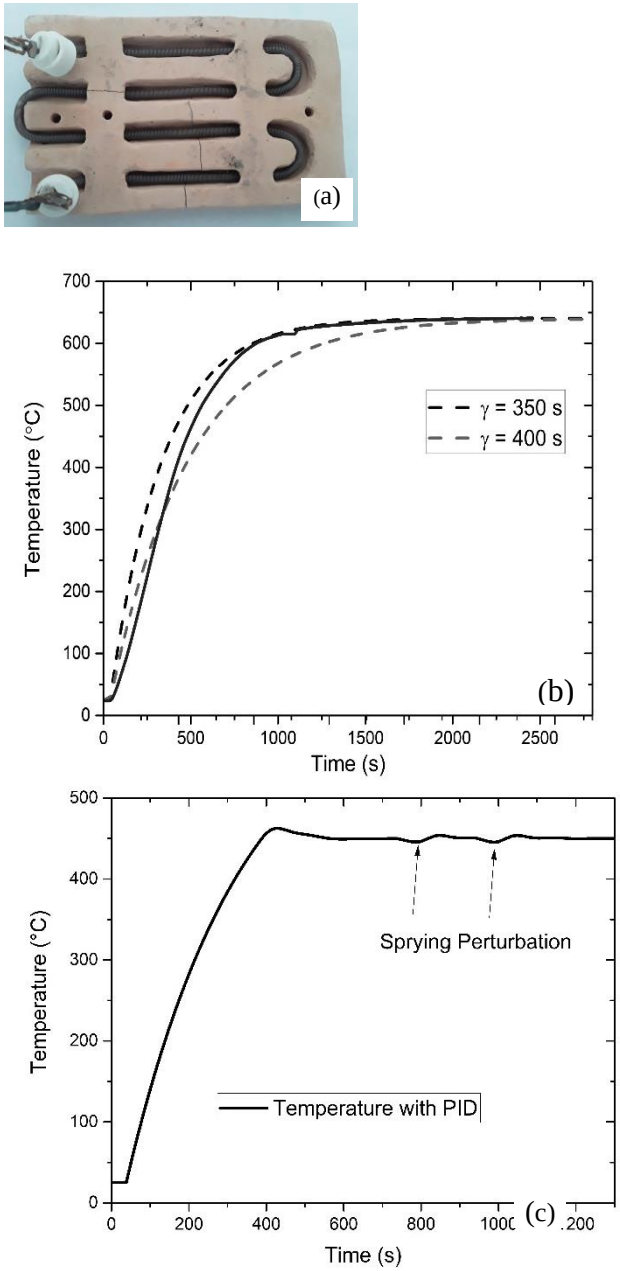

Figure 6. (a) Elastic resistance embedded in ceramic mount (b) Experimental (solid line) and simulated open-loop response (c) Simulated output signal response of the close loop system with spraying perturbations.

gives 25±8 W. By incorporating a perturbation due to a continuous spray of a duration of 60 s, the obtained time response is presented in Figure 7. An oscillation of about 5 °C is observed during the spraying time because supplied power cannot immediately compensate for this loss. This temperature variation can affect the manufacturing process. To overcome this issue is required more power supply or an intermittently spraying or other modification to keep the temperature constant during spraying.

B-Flow sensing

During the deposition, three processing steps take place: the atomization of the precursor solution; aerosol transport of the droplet; decomposition of the precursor to initiating film growth. In the former, the solution is pulverized and transformed in droplets which acquire a velocity. In these processes, the droplets are subjected to different actuating forces that modify the initial velocity obtained in the outer diameter of the nozzle. The initial pressure of the carrier gas will modify the droplet radius and the initial velocity. It is reported [8] that most of the droplet's trajectory is distributed within a cone of 70° and the half of them are within 12°, the pressure of the carrier gas was of 2 bar and a nozzle outer diameter is 0.1 mm.

The cone of pulverized droplets and its radius should be maintained quite stable and in a stationary regime. This fact can be disturbed by almost three factors: agglomeration of material in the nozzle, a slight variation in the flow pressure, a variation of the solution in the reservoir, manual, or automatized movement of the airbrush. To ensure a homogeneous deposition it is important to measure the characteristic of the flow cone. If the nozzle is maintained fixed, this can be implemented by measuring in some fixed points the local velocity with hot wire anemometry method, also laser anemometry doppler can be introduced to probe the velocity and particle size [9,10]. An electrical solenoid valve will control the flux of carrier gas, this valve will stop the flow when the substrate temperature decreases, or the sensed properties are not acceptable. Also, by controlling this valve different frequencies of the pulsed carrier gas can be applied to obtain different manufacturing conditions.

B. Different integration configurations

As mentioned in the previous section, the flow should not be continuously applied because it makes a decrease in the operating temperature that the power supply cannot compensate and the material is not adequately sintered, leading to an inhomogeneous resulting film. We considered that are almost three possible responses to this issue and are shown in Figure 8, (i) applying a pulsed flow controlled by a solenoid electrical valve, (ii) produce a continuous movement of the thermal set, or (iii) produce a continuous movement of the spraying nozzle. The first option could lead to a non-homogenous result because in each pulse the starting droplets differ from the regime condition, but it only requires opening and closing the carrier gas valve, so it is an interesting fact to be incorporated. The second option presents the difficulty of moving a complete thermal set over a rail employing a step by step DC electrical motor, and the flow is maintained stable and the decrease of substrate temperature can be also controlled with the translation velocity. This configuration could lead to a stable process and thus, homogenous films. The third configuration can be easier than moving the complete set of the thermal component, but the flow will change continuously when the nozzle is moved, so, like in the first option the obtained films can be inhomogeneous. The final design is composed of a moving thermal component and pulsed spraying simultaneously, i.e., a combination of configurations (i) and (iii).

Finally, we present a design of the whole system summarized in the blocks diagram presented in Figure 9. In this design, the whole spray pyrolysis system is controlled by an Arduino hardware.

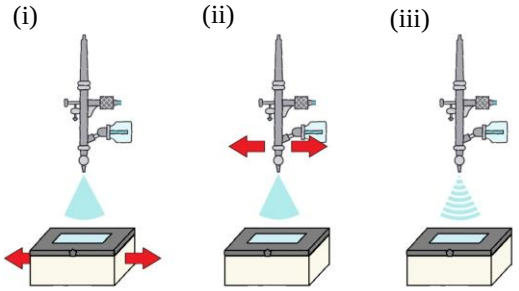

Figure 8. Scheme of integration configurations.

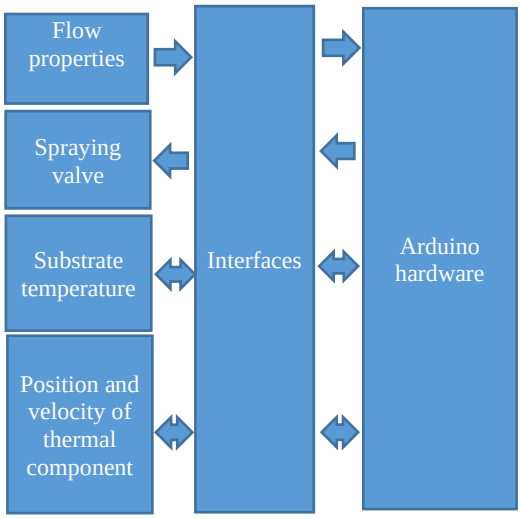

Figure 9. Diagram of the complete spray pyrolysis system.

III. Conclusions

In this paper, we have simulated some parameters of a low-cost design of a spray pyrolysis instrument. We present relevant characteristics of this system and experimental results of temperature variation for different modes of a commercial temperature controller and two different thermal plants. By formulating the mathematical model of the first thermal component, the bandwidth and time response of this subsystem were simulated and analyzed in different operation conditions, so a PID was designed to carry out a low-cost thermal control, to replace the commercial one. Then a second thermal component was evaluated in open-loop condition and simulated. In this, the spraying perturbation was simulated, and it was concluded that the heat flux supplied by the resistance is not enough to maintain the setpoint value during operation. To avoid this fact, different configurations of the equipment were analyzed, and an overcomer solution is proposed.

Summarizing, we presented a low-cost design for automatized spray pyrolysis technique to manufacture high quality semiconductor layers. These are relevant materials to develop LEDs, solar cells, and selective optical filters. In the future, a detailed assembly of this system will be approach and the different resulting films will be inquired.

Acknowledgment

MO wish to thanks to Consejo Interuniversitario Nacional (CIN) for the scholarship. This paper was partially supported

by Quilmes National University under contract PUNQ #1303/19.

REFERENCES

[1] Brinker, C. Jeffrey Brinker, Alan Hurd, Fundamentals of sol-gel dip-coating, Journal de Physique III, 7 (1994) 1231.

[2] Giancarlo C. Righini, Chapter: Characterization of Sol–Gel Thin-Film Waveguides, Handbook of Sol-Gel Science and Technology; Kubler Academic Publishers, 2016.

[3] R.M. Pasquarelli, D.S. Ginley, R.O'Hayre, Solution processing of transparent conductors: from flask to film, Chem. Soc. Rev. 40 (2011) 55406.

[4] L. Znaidi, Sol–gel-deposited ZnO thin films: A review, Mat. Sci. Eng. B 174 (2010) 18.

[5] M. R. Tejerina, M. Gamba, L. Ponce, F. Alvira. Comparative analysis of TiO2 layers grown by pulsed laser deposition at atmospheric pressure and pyrolitic nebulization. Optica Pura y Aplicada. 51 (2018) 1-7 (2018) 50301.

[6] www.engineeringtoolbox.com https://www.engineeringtoolbox.com/convective-heat-transfer-d_430.html#:~:text=Typical%20convective%20heat%20transfer%20coefficients,%2F(m2K))

[7] F., & Salgado, M. E. (2001). Control system design. Upper Saddle River, NJ: Prentice Hall.

[8] L. Filipovic, S. Selberherr, C. G. Mutinati, E. Brunet, S. Steinhauer, A. Köck, J. Teva, J. Kraft, J. Siegert, F. Schrank (2013). Modeling Spray Pyrolysis Deposition. Lecture Notes in Engineering and Computer Science. 2. 987-992.

[9] Yan, Zhibin & Zhao, Rui & Duan, Fei & Wong, Teck & Toh, Kok & Choo, Kok & Chan, Poh & Chua, Yong. (2011). Spray Cooling. 10.5772/21076.

[10] Pais M.R., Chow L.C., Mahefkey E.T., Surface roughness and its effect on the heat transfer mechanism in spray cooling, Journal of Heat Transfer, Vol. 114, pp. 211–219 (1992)